Journal of Science and Technology in Civil Engineering, NUCE 2020. 14 (3): 75–83

TWO-SCALE DESIGN OF POROSITY-LIKE MATERIALS USING ADAPTIVE GEOMETRIC COMPONENTS

Van-Nam Hoang[a,*]

[a]*Mechanical Engineering Institute, Vietnam Maritime University, Hai Phong city, Vietnam*

Article history:
Received 03/06/2020, Revised 07/08/2020, Accepted 10/08/2020

Abstract

This paper is an extension of our recent work that presents a two-scale design method of porosity-like materials using adaptive geometric components. The adaptive geometric components consist of two classes of geometric components: one describes the overall structure at the macrostructure and the other describes the structure of the material at the microstructures. A smooth Heaviside-like elemental-density function is obtained by projecting these two classes on a finite element mesh, namely fixed to reduce meshing computation. The method allows simultaneous optimization of both the overall shape of the macrostructure and the material structure at the micro-level without additional techniques (i.e., material homogenization), connection constraints, and local volume constraints, as often seen in most existing methods. Some benchmark structural design problems are investigated and a selected design is post-processed for 3D printing to validate the effectiveness of the proposed method.

Keywords: topology optimization; concurrent optimization; porosity structures; two-scale topology optimization; adaptive geometric components.

https://doi.org/10.31814/stce.nuce2020-14(3)-07

1. Introduction

Porosity-like materials that exist in nature have exceptionally high strength for their own weight [1, 2]. Trabecular bones and beehives represent the structures of such materials (Fig. 1). In addition to high strength-to-mass ratios, this kind of material is also capable of diffusion of fluid media [3, 4], energy absorption, and shock resistance [5, 6]. Especially in some medical cases, porous materials require diffusion of liquids through themselves. Regarding the two-scale topology optimization or concurrent topology optimization [4, 7–14] of porosity-like materials, most of the existing methods are mainly based on the material homogenization technique [15]. Accordingly, the design domain is divided into a finite number of macro elements, each of which is a microstructure that is subdivided into a finite number of microelements and designed independently. The geometries of a microstructure are used to approximate the mechanical properties of the macro element through material homogenization. In each optimization loop, the finite element analysis and new variable updates are required at two levels, macro and microstructures, which require a lot of calculations. Besides, some constraints on the connection between macro elements and local volume constraints to ensure structural porosity are also needed, leading to memory consumption. (see [12] for a short review of concurrent designs).

Recently, Hoang and his collaborators have proposed a direct two-scale topology optimization method for honeycomb-like structures [17] using adaptive geometric components, which is inspired

*Corresponding author. *E-mail address:* namhv.vck@vimaru.edu.vn (Hoang, V. N.)

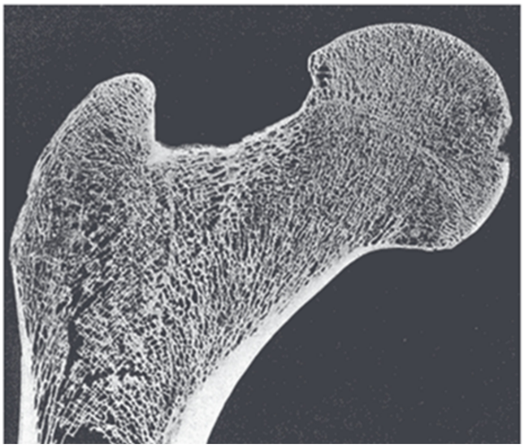

(a) Trabecular bone by [3]

(b) Honeycomb by [16]

Figure 1. Porosity-like structures

by moving morphable bar method [18, 19]. The method allows straightforwardly optimizing macro and microstructures through searching a set of geometry parameters (including macro and micro parameters) without the use of material homogenization techniques and additional constraints. Two-scale model using adaptive geometric components was also extended to the design of lattice structures [20] and coated structures with nonperiodic infill [21]. In this paper, we briefly review the projection technique of adaptive geometric components for non-uniform honeycomb-like structure optimization and extend the proposed method for flexible designs of porosity-like materials. In which, non-moving micro void circles in [17] are replaced by moving micro void bars to enhance degrees of freedom in optimization design.

In the scope of this paper, the developed scheme is limited to two-dimensional (2D) design problems. To extend the current method for three-dimensional (3D) problems, readers are recommended to refer to moving morphable patch method [22] which aims to full-thickness control of 3D structural optimization, and extruded geometric component method [23] where an adaptive mapping technique was employed to enhance computational efficiency and 2D calculations could be replaced for 3D calculations. A Matlab code for extruded-geometric-component-based 3D topology optimization is available at [24].

2. Adaptive geometric components

The adaptive geometric components consist of two classes of geometric components: one consisting of macro moving bars describes the macrostructure and the other consisting of micro void circles describes the microstructure [17]. Each macro bar is described by the positions of endpoints $\mathbf{x}_{k1}, \mathbf{x}_{k2}$ and its thickness $2r_k$ and each micro circle is described by the position $\mathbf{x}_m$ and its radius r_m (see Fig. 2(a)). Mapping these two classes of geometric components onto the finite element mesh yields the element density field ρ_e as illustrated in Fig. 2(a). In which, element density $\rho_e = 1$ (solid) if the element locates both inside the macro bars and outside the micro circles, $\rho_e = 0$ (void) if the element locates outside macro bars or inside micro circles, and $0 < \rho_e < 1$ if the element locates around the structural boundaries.

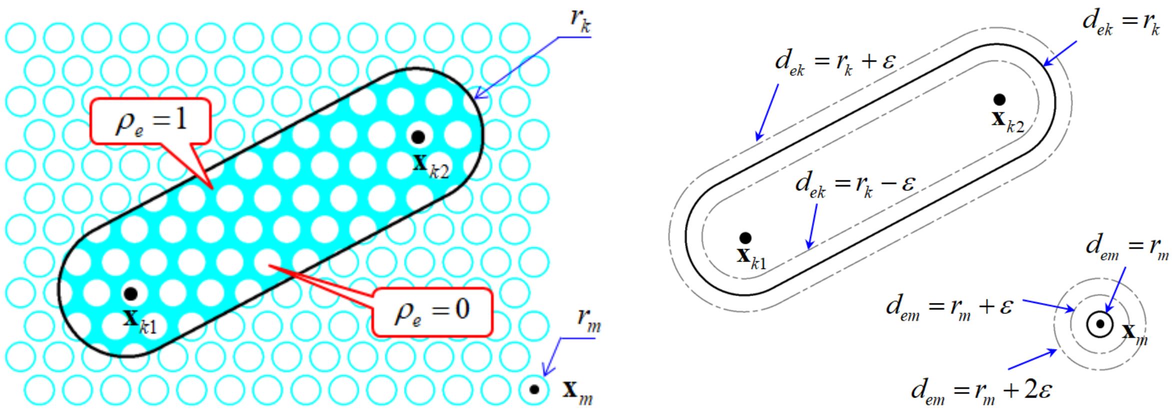

(a) (b)

Figure 2. Mapping adaptive geometric components: (a) solid material is highlighted in cyan, (b) level sets of the minimum distance functions (d_{ek}, d_{em}) are illustrated with ε being a positive number

The element density function is given by

$$\rho_e = (1 - \phi_{ma})\phi_{mi} \tag{1}$$

where ϕ_{ma} is obtained by projecting the macro bars onto the mesh and ϕ_{mi} is obtained by projecting the micro circles onto the mesh, expressed as follows

$$\phi_{ma} = \prod_{k=1}^{M_a} \frac{1}{1 + \exp[-\beta(d_{ek} - r_k)]} \tag{2}$$

$$\phi_{mi} = \prod_{m=1}^{M_i} \frac{1}{1 + \exp[-\beta(d_{em} - r_m)]} \tag{3}$$

where d_{ek} and d_{em} represent the minimum distances from element e to the center axis of macro bar k and the center of micro circle m, respectively (Fig. 2(b)); M_a and M_i denote the number of macro bars and micro circles, respectively and β is a positive control parameter [18, 25].

3. Two-scale designs of porosity-like structures

The goal is to find a set of geometry parameters $\mathbf{x} = \{\mathbf{x}_{k1}, \mathbf{x}_{k2}, r_k, r_m\}, k = 1, 2, ..., m = 1, 2, ...$ so that the overall stiffness is as close as possible to the maximum. This leads to a compliance minimal problem, given by

$$\begin{aligned} &\min_{\mathbf{x}} c(\mathbf{x}) = \sum_{e=1}^{N} \chi \mathbf{d}_e^T \mathbf{k}_0 \mathbf{d}_e \\ &\text{subject to } \frac{1}{|\Omega_0|} \int_{\Omega_0} \rho_e d\Omega - f \leq 0 \\ &\mathbf{x}_{\min} \leq \mathbf{x} \leq \mathbf{x}_{\max} \end{aligned} \tag{4}$$

where c represents the structural compliance; N is the number of elements of the finite element mesh; $\mathbf{k}_0$ denotes the element stiffness matrix; $\mathbf{d}_e \subset \mathbf{d}$ is the element displacement vector; $|\Omega_0|$ denotes the design-domain volume; f denotes the volume fraction; $\mathbf{x}_{\min}, \mathbf{x}_{\max}$ are the bounds of the design variable vector $\mathbf{x}$; and $\mathbf{d}$ is the global displacement vector, obtained by solving the following equation,

$$\mathbf{Kd} = \mathbf{F} \tag{5}$$

where $\mathbf{K}$ and $\mathbf{F}$ correspond to the global stiffness matrix and force vector, respectively.

The characteristic function χ in Eq. (4) is defined as in the isotropic material with penalization (SIMP) [26],

$$\chi = \rho_{\min} + \rho_e^{\eta}(1 - \rho_{\min}) \tag{6}$$

where $\eta = 3$ is the penalization parameters and $\rho_{\min} = 10^{-4}$ is a small positive number for numerical treatment.

4. Examples

4.1. Non-uniform honeycomb problem with fixed-position void circles

In this subsection, the design of a simply supported beam is investigated. The design definitions are given in Fig. 3, in which a rectangular design domain is described with dimensions 150×50, fixed horizontal degrees of freedoms of the left side, fixed vertical degree of freedoms of the lower right point, and unit load on the top-left. The design problem is solved in the plane-stress state using 300×100 four-node elements and volume fraction $f = 0.5$. The base material is assumed to be homogeneous with Young's modulus $E_0 = 1$ and Poisson's ratio $\nu_0 = 0.3$.

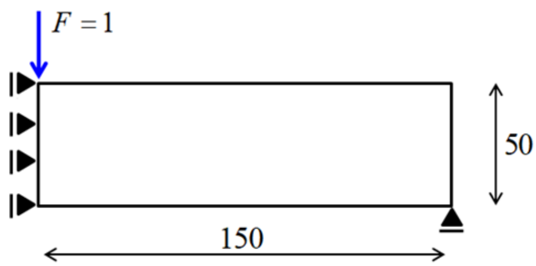

Figure 3. Simply supported beam design definitions

Firstly, the moving-morphable-bars-based method [18] is employed to optimize the beam with solid material. The initial layout of 48 moving morphable bars is employed (Fig. 4(a)). The problem is solved with a 50% material volume of the design domain volume by moving material blocks (moving morphable bars) in the design domain and changing their thicknesses. The optimized layout of moving morphable bars is presented in Fig. 4(b) and the optimized design is plotted in Fig. 4(c). This is the optimum shape of the beam that we often see in the literature.

Now, we apply the projection technique of adaptive geometric components in topologically optimizing the beam with porosity-like material. The initial layout of adaptive geometric components is given in Fig. 5(a), where we use 48 marco bars and 335 micro circles corresponding to 575 geometry parameters. The problem is solved by straightforwardly optimizing the geometry parameters of adaptive geometric components. As expected, a design with porosity is successfully achieved on a coarse mesh of 300×100 elements as shown in Fig. 5(c). Fig. 5(b) plots optimized geometries of adaptive geometric components.

It is worth noting that the proposed method uses a dramatic reduction of design variables, i.e., 575 design variables in the current example compared to dozen million design variables if the homogenization-based conventional methods such as SIMP or level set methods is used [14]. Whereas the

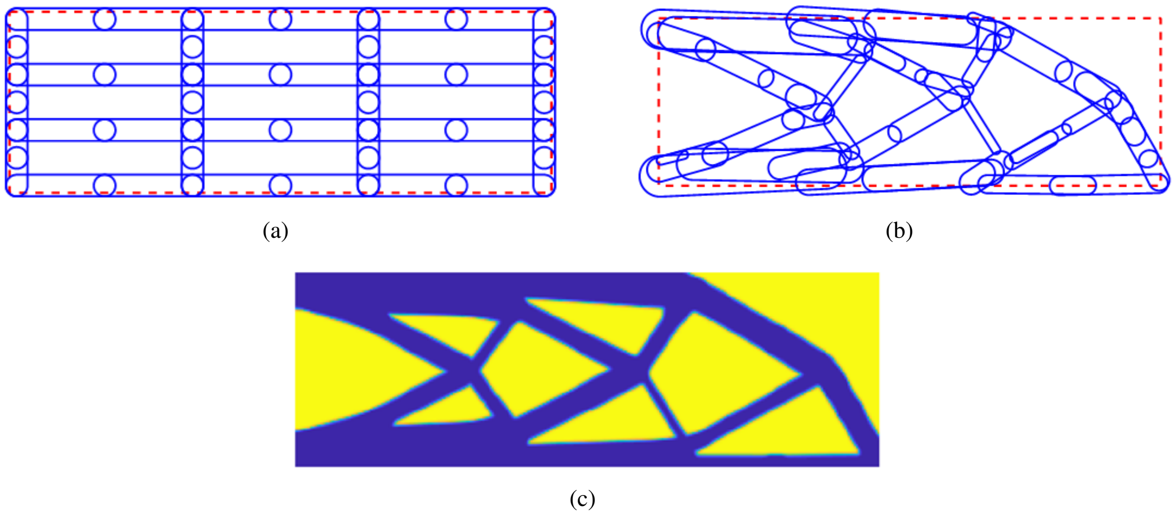

Figure 4. Simply supported beam: (a) initial layout of moving morphable bars, (b) optimized layout of moving morphable bars, (c) optimized design of solid material (material zones are highlighted in blue, void zones are highlighted in yellow)

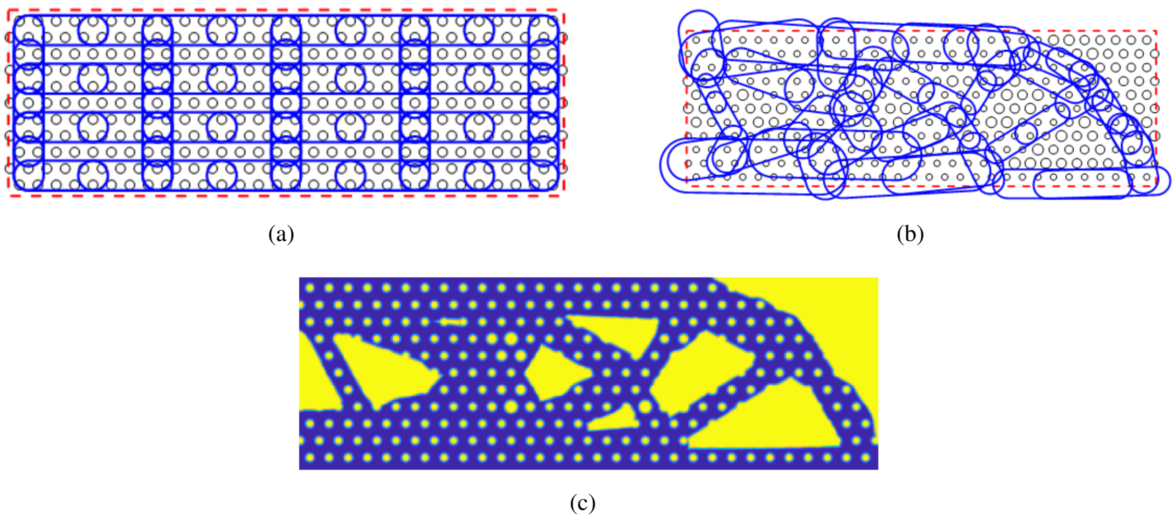

Figure 5. Porosity-like structure [17]: (a) initial layout of adaptive geometric components, (b) optimized layout of adaptive geometric components, (c) optimized design

homogenization technique, connector constraints, and local volume constraints are not required in the proposed method. This also means that the proposed method requires less storage space. Although we can not provide a truly fair comparison of the proposed method with others because of the differences in the problem definitions, kinds of used computers, and selected design-parameters. But it is clear that the use of fewer design variables, the absence of homogenization techniques, and local volume and connectivity constraints will reduce computational and storage costs. The convergence criterion usually reaches after about 100 loops with a period of several minutes, cheaper than the costs in [12] (hourly to dozens of hours).

The design in Fig. 5(c) is post-processed for STL format to be printed on Zortrax M200 Plus printing machine. The printing result, which is shown in Fig. 6, confirms the possibility of realizing the two-scale design of porous materials using adaptive geometric components for additive manufacturing techniques. It's worth remarking that the material continuity of microstructures and the porosity of each microstructure can be ensured without additional constraints. The minimum thickness of members of the microstructures, which is to ensure the ability to fabricate by 3D printers, can also be straightforwardly controlled by the selection of thickness parameters of micro circles (see [17, 20] for more details).

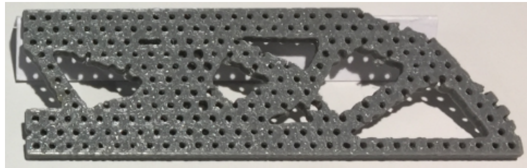

Figure 6. 3D printing result of the design sample with bounded dimensions $150 \times 50 \times 3$ (mm)

4.2. *Non-uniform honeycomb problem with moving void bars*

In this subsection, we extend the proposed method for other types of micro geometric components to enhance degrees of freedom in optimization design. In this situation, fixed micro circles in the above examples are replaced by moving micro bars (Fig. 7(a) and 7(b)). Each micro bar plays like a moving void component that can be move and change its orientation and thickness in a local domain belonging to the design domain Ω_0. Once again, a porosity-like design is obtained by searching an optimal set of macro and micro geometry parameters without the homogenization and additional constraints. The optimized porous design is shown in Fig. 7, in which Fig. 7(b) plots optimized adaptive geometric components and Fig. 7(c) plots optimized design in the element density field.

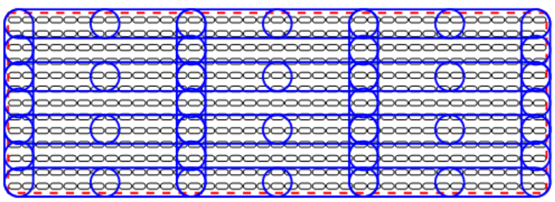

(a) Initial layout of adaptive geometric components

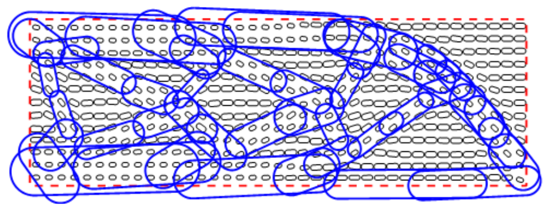

(b) Optimized layout of adaptive geometric components

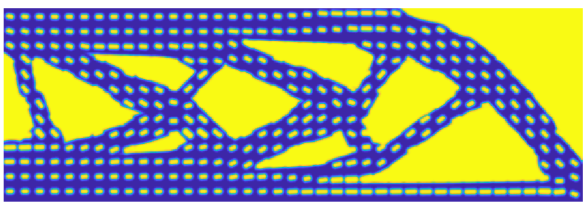

(c) Optimized design

Figure 7. Simply supported beam design with micro moving void bars

Finally, we employ the proposed method for simultaneously optimizing the macro structure and micro material structures of a cantilever beam under a unit load as defined in Fig. 8. The design domain with dimensions 40×80 is discretized with 160×320 plane-stress elements. The base material is assumed to be homogeneous with unit Young's modulus and Poisson's ratio $\nu_0 = 0.3$. Two cases with different allowed volumes of the design material are considered: one is 30% volume of the design domain and the other is 40% volume of the design domain. Fig. 9 shows the optimized designs with solid material, and Fig. 10 shows the optimized designs with porous material.

As expected, the overall structural topology and micro material structures can be optimized at the same time by straightforwardly optimizing the geometries of the adaptive geometric components while the optimizer does not require the homogenization technique. The continuity of material microstructures and their porosities are always ensured without connection constraints and local volume constraints. It's noted that the values of objective functions of the solid design in Fig. 9 are smaller than those of the porous design in Fig. 10. In other words, the solid design is stiffer than the porous design. This is in agreement with [10], in which with the same volume of material, the less porosity, the higher stiffness; the solid structure has higher stiffness than the porous one does.

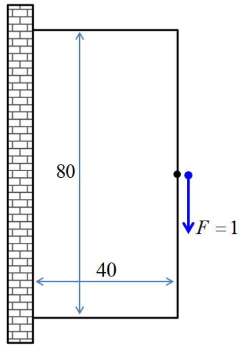

Figure 8. Cantilever beam with design definitions

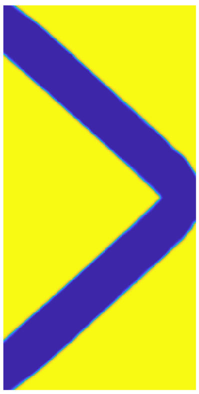

$c = 9.10$

(a) Optimized design with $f = 0.3$

$c = 7.51$

(b) Optimized design with $f = 0.4$

Figure 9. Cantilever beam optimization with solid material

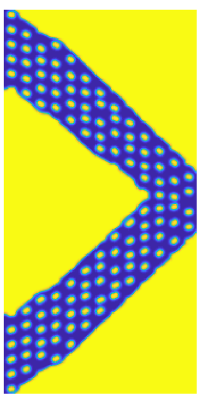

$c = 16.05$

(a) Optimized design with $f = 0.3$

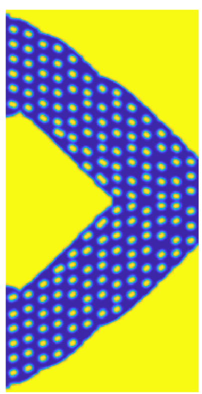

$c = 12.92$

(b) Optimized design with $f = 0.4$

Figure 10. Cantilever beam optimization with porous material

5. Conclusions

A straightforward topology optimization method of porosity-like materials was proposed by using adaptive geometric components consisting of two classes of geometric components. The overall topology of the macrostructure and the microstructures are simultaneously optimized by searching an optimal set of macro and micro geometry parameters without material homogenization, connector constraints, and local volume constraints. Some benchmark structural problems were investigated and a selected design was post-processed for 3D printing to validate the effectiveness of the proposed method.

In this paper, the finite element method was employed for structural analysis and the moving morphable bar method was applied for structural optimization. In the near future, a combination of isogeometric analysis [27, 28] and moving polygonal morphable voids [29] in the design of porous materials will be explored.

Acknowledgments

This research is funded by Vietnam National Foundation for Science and Technology Development (NAFOSTED) under grant number 107.01-2019.317.

References

[1] Gibson, L. J., Ashby, M. F. (1997). *Cellular solids: Structure and properties*. Second edition, Cambridge University Press.

[2] Christensen, R. M. (2000). Mechanics of cellular and other low-density materials. *International Journal of Solids and Structures*, 37(1-2):93–104.

[3] Wang, X., Xu, S., Zhou, S., Xu, W., Leary, M., Choong, P., Qian, M., Brandt, M., Xie, Y. M. (2016). Topological design and additive manufacturing of porous metals for bone scaffolds and orthopaedic implants: A review. *Biomaterials*, 83:127–141.

[4] Svanberg, K. (1987). The method of moving asymptotes—a new method for structural optimization. *International Journal for Numerical Methods in Engineering*, 24(2):359–373.

[5] Elnasri, I., Pattofatto, S., Zhao, H., Tsitsiris, H., Hild, F., Girard, Y. (2007). Shock enhancement of cellular structures under impact loading: Part I Experiments. *Journal of the Mechanics and Physics of Solids*, 55 (12):2652–2671.

[6] Ajdari, A., Nayeb-Hashemi, H., Vaziri, A. (2011). Dynamic crushing and energy absorption of regular, irregular and functionally graded cellular structures. *International Journal of Solids and Structures*, 48 (3-4):506–516.

[7] Deng, J., Yan, J., Cheng, G. (2012). Multi-objective concurrent topology optimization of thermoelastic structures composed of homogeneous porous material. *Structural and Multidisciplinary Optimization*, 47 (4):583–597.

[8] Xia, L., Breitkopf, P. (2014). Concurrent topology optimization design of material and structure within FE2 nonlinear multiscale analysis framework. *Computer Methods in Applied Mechanics and Engineering*, 278:524–542.

[9] Vicente, W. M., Zuo, Z. H., Pavanello, R., Calixto, T. K. L., Picelli, R., Xie, Y. M. (2016). Concurrent topology optimization for minimizing frequency responses of two-level hierarchical structures. *Computer Methods in Applied Mechanics and Engineering*, 301:116–136.

[10] Sivapuram, R., Dunning, P. D., Kim, H. A. (2016). Simultaneous material and structural optimization by multiscale topology optimization. *Structural and Multidisciplinary Optimization*, 54(5):1267–1281.

[11] Yan, J., Guo, X., Cheng, G. (2016). Multi-scale concurrent material and structural design under mechanical and thermal loads. *Computational Mechanics*, 57(3):437–446.

[12] Xia, L., Breitkopf, P. (2016). Recent Advances on Topology Optimization of Multiscale Nonlinear Structures. *Archives of Computational Methods in Engineering*, 24(2):227–249.
[13] Deng, J., Chen, W. (2017). Concurrent topology optimization of multiscale structures with multiple porous materials under random field loading uncertainty. *Structural and Multidisciplinary Optimization*, 56(1):1–19.
[14] Li, H., Luo, Z., Gao, L., Qin, Q. (2018). Topology optimization for concurrent design of structures with multi-patch microstructures by level sets. *Computer Methods in Applied Mechanics and Engineering*, 331:536–561.
[15] Bendsøe, M. P., Kikuchi, N. (1988). Generating optimal topologies in structural design using a homogenization method. *Computer Methods in Applied Mechanics and Engineering*, 71(2):197–224.
[16] Honeycomb. *https://sonlamfood.com/*.
[17] Hoang, V.-N., Nguyen, N.-L., Tran, P., Qian, M., Nguyen-Xuan, H. (2020). Adaptive Concurrent Topology Optimization of Cellular Composites for Additive Manufacturing. *JOM*, 72(6):2378–2390.
[18] Hoang, V.-N., Jang, G.-W. (2017). Topology optimization using moving morphable bars for versatile thickness control. *Computer Methods in Applied Mechanics and Engineering*, 317:153–173.
[19] Wang, X., Long, K., Hoang, V.-N., Hu, P. (2018). An explicit optimization model for integrated layout design of planar multi-component systems using moving morphable bars. *Computer Methods in Applied Mechanics and Engineering*, 342:46–70.
[20] Hoang, V.-N., Tran, P., Vu, V.-T., Nguyen-Xuan, H. (2020). Design of lattice structures with direct multiscale topology optimization. *Composite Structures*, 252:112718.
[21] Hoang, V.-N., Tran, P., Nguyen, N.-L., Hackl, K., Nguyen-Xuan, H. (2020). Adaptive Concurrent Topology Optimization of Coated Structures with Nonperiodic Infill for Additive Manufacturing. *Computer-Aided Design*, page 102918.
[22] Nguyen, H.-D., Hoang, V.-N., Jang, G.-W. (2020). Moving morphable patches for three-dimensional topology optimization with thickness control. *Computer Methods in Applied Mechanics and Engineering*, 368:113186.
[23] Hoang, V.-N., Nguyen-Xuan, H. (2020). Extruded-geometric-component-based 3D topology optimization. *Computer Methods in Applied Mechanics and Engineering*, 371:113293.
[24] Github. *EGC_3dTOP.SIMOGroup*. Visited on 03/08/2020.
[25] Hoang, V.-N., Nguyen, N.-L., Nguyen-Xuan, H. (2019). Topology optimization of coated structure using moving morphable sandwich bars. *Structural and Multidisciplinary Optimization*, 61(2):491–506.
[26] Bendsøe, M. P. (1989). Optimal shape design as a material distribution problem. *Structural Optimization*, 1(4):193–202.
[27] Hughes, T. J. R., Cottrell, J. A., Bazilevs, Y. (2005). Isogeometric analysis: CAD, finite elements, NURBS, exact geometry and mesh refinement. *Computer Methods in Applied Mechanics and Engineering*, 194(39-41):4135–4195.
[28] Lieu, N. T. B., Hung, N. X. (2019). Static analysis of piezoelectric functionally graded porous plates reinforced by graphene platelets. *Journal of Science and Technology in Civil Engineering (STCE) - NUCE*, 13(3):58–72.
[29] Van-Nam, H. (2020). An explicit topology optimization method using moving polygonal morphable voids (MPMVs). *Science and Technology Development Journal*, 23(2):536–540.